REPORT DOCUMENTATION PAGE

Form Approved
OMB No. 0704-0188

1. AGENCY USE ONLY (Leave Blank)	2. REPORT DATE 17 Dec. 1998	3. REPORT TYPE AND DATES COVERED Final Technical Report

4. TITLE AND SUBTITLE	5. FUNDING NUMBERS
Integrated Electric Actuator Application to Flight Control Technology	F33615-98-C-3604

6. AUTHOR(S)
Natalie Hammer
Charles B. Bright

7. PERFORMING ORGANIZATION NAME(S) AND ADDRESS(ES) ETREMA Products, Inc. 2500 North Loop Drive Ames, IA 50010	8. PERFROMING ORGANIZATION REPORT NUMBER N/A
9. SPONSORING/MONITORING AGENCY NAME(S) AND ADDRESS(ES) Air Force Research Laboratory 2530 C Street Wright-Patterson AFB, OH 45433-7607	10. SPONSORING/MONITORING AGENCY REPORT NUMBER Delivery item 0001

11. SUPPLEMENTARY NOTES

19990119 075

12a. DISTRIBUTION/AVAILABILITY STATEMENT
Approved for public release, ~~SBIR report~~ distribution unlimited

13. ABSTRACT (Maximum 200 words)
This report summarizes the work accomplished during SBIR AF98-175, "Integrated Electric Actuator Application to Flight Control Technology." ETREMA Products, Incorporated refers to this program as the Vulkan^{TM} IEA program or as the IEA.
The development of an IEA is key to achieving lighter, simpler, more reliable, and more cost-effective vehicle control systems. Phase I focused on modeling to demonstrate the feasibility of the IEA to produce sufficient fluid flow at sufficient pressure to perform work. TERFENOL-D transducers drove a piston, an inlet poppet valve, and an outlet poppet valve. Predicted fluid output power peaked at 632 watts (0.85 hp). Active valve controllability is a significant challenge.

14. SUBJECT TERMS	15. NUMBER OF PAGES
Integrated Electric Actuator, TERFENOL-D	21
	16. PRICE CODE

17. SECURITY CLASSIFICATION OF REPORT Unclassified	18. SECURITY CLASSIFICATION OF THIS PAGE Unclassified	19. SECURITY CLASSIFICATION OF ABSTRACT Unclassified	20. LIMITATION OF ABSTRACT UL

NSN 7540-01-280-5500   (Facsimile)

Standard Form 298 (Rev. 2-89)
Prescribed by ANSI Std. Z39-18
298-102

Technical Report for Phase I SBIR Topic #AF98-175:

"Integrated Electric Actuator Application to Flight Control Technology"

December 17, 1998

ETREMA Products, Incorporated
,2500 North Loop Drive
Ames, Iowa, USA 50010-8278
Telephone 515.296.8030
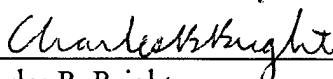
Prepared By: _____   12/17/98
Natalie Hammer   Date
Design Engineer
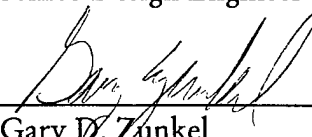
Prepared By: _____   17DEC98
Charles B. Bright   Date
Senior Design Engineer

Approved By: _____   12/17/98
Gary D. Zunkel   Date
Director of Engineering

TABLE OF CONTENTS

LIST OF FIGURES

LIST OF TABLES

Abstract

This report summarizes the work accomplished during SBIR AF98-175, "Integrated Electric Actuator Application to Flight Control Technology." ETREMA Products, Incorporated refers to this program as the Vulkan™ IEA program or as the IEA.

The development of an IEA is key to achieving lighter, simpler, more reliable, and more cost-effective vehicle control systems. Phase I focused on modeling to demonstrate the feasibility of the IEA to produce sufficient fluid flow at sufficient pressure to perform work. TERFENOL-D transducers drove a piston, an inlet poppet valve, and an outlet poppet valve. Predicted fluid output power peaked at 632 watts (0.85 hp). Active valve controllability is a significant challenge.

I. Introduction

Hydraulic power is the preferred method of gaining mechanical advantage for use within an aircraft. Hydraulic power provides the mechanical muscle to operate existing loads such as primary flight controls, flaps, slats, landing gear retraction and extension, brakes and steering, thrust reversers, and weapons bay doors. Hydraulic power distribution involves routing fluid supply and return lines to connect sources to loads throughout the airframe. This exposes these lines to multiple failure means. It follows that pressurized fluid containment failure probabilities dictate redundancy requirements, leading to multiple systems with redundant components and cross-coupling. Redundant components and cross-coupling do not fulfill the primary task of providing pressurized fluid to a load but exist to reduce aircraft vulnerability to fluid loss at the price of additional weight, cost, and maintenance. Another significant problem created by long hydraulic lines and fast flight controls is water hammer. This can shorten component life through fatigue. For example, in one jetliner, water hammer appeared due to fast flight control dynamics, and was corrected by adding accumulators with non-negligible weight. Conventional solutions to fluid dynamics problems often involve adding components or strengthening components (additional weight and cost) to increase their fatigue life.

Hydraulic power originates at a pump driven by a sufficiently powerful mechanical means. This involves driving a pump directly from a rotating engine, bleeding engine compressed air to drive an air turbine, using an electrical motor powered by an engine generator, using one hydraulic system to pressurize another through a motor/pump arrangement, an emergency ram air turbine, or using a helium bottle for a short duration. These sources of mechanical power are not necessarily co-located with the end use, such as aircraft control surface actuators. Therefore, the hydraulic power must be distributed from a central source. Co-locating a hydraulic power source with its end use, especially as a unitized module, retains the fluid power advantages while reducing the total size and complexity of hydraulic fluid containment and can relieve some fluid dynamics problems caused by high response requirements.

Current state-of-the-art solutions that locate the pressure source near the load use the electrical system as a power source.[1] Electrical systems are ubiquitous, flexible, and power distribution wiring is relatively small, lightweight, and survivable compared to fluid lines or bleed air ducts. The electrical power is converted to fluid power using a conventional rotating electric motor to drive a pump. This package, while offering certain advantages, has rotational inertia, bearings to wear out, current inrush, sensitivity to low voltage, and weight and bulk.[2,3,4,5] Further, unidirectional pump output requires valving to change output direction.

In the context of this report, the undesirable dynamics due to rotating inertia originate in the basic construction of a hydraulic pump and its electric drive motor.[6] Accelerating the electric motor, pump cylinder block, and other essential parts from rest requires a large amount of current relative to steady-state operation. This is because electric motor impedance is a function of speed and power is drawn and converted into rotational energy. Accelerating against a mechanical load inevitably either slows down acceleration, thus delaying response, or requires additional current, which may burn out the motor if voltage droops unexpectedly. If acceleration is to be quick enough, power wiring weight must increase to support current inrush requirements.

In contrast, the proposed Integrated Electric Actuator (IEA) concept offers the ability to overcome these disadvantages while offering the same advantages in a simpler, "miniature," unitized module. Its substantially reduced inertia enables quick response. It has no need for sliding bearings, eliminates start-up current inrush, and may use variable voltage to control its output. Electronic valve control may provide bi-directional pumping action, eliminating the servovalve used to port pressurized fluids. This level of valve control can be configured to provide an inherent fail-safe position, soften pressure pulsations and change valve motion according to the requirements of various flight regimes. The basic IEA configuration also offers the Air Force advantages of lower weight, reduced cost, longer life, better contamination resistance, improved maintainability, and increased reliability.

II. Software Model Development

To determine the feasibility of the IEA concept, a dynamic model coupled with results from a lumped parameter model was created. Modeling the physical situation requires defining numerical parameters which in turn requires a layout of roughly what the IEA would look like. Figures II-1 and II-2 define the chosen fluid path geometry configuration, including the "squeeze film damping relief channels" similar to information found in Air Force report WRDC-TR-90-3074 (used with permission). From these figures, the appropriate force balances, etc. can be derived.

1. "Designing Electrically Powered Actuators for Aircraft," NASA Tech Briefs, 10/97, P 84.
2. "Advanced Actuator Tested On F/A-18," Aviation Week & Space Technology, February 12, 1996, P 42.
3. "Aerospace Climbs Higher With Fluid Power," Design News, July 20, 1992, P 55.
4. "'Electric' Ailerons Subject Of Air Force C-141 Tests," Aviation Week & Space Technology, May 6, 1996, P 52.
5. "Aircraft Hydraulic Systems," Aerospace Engineering, March, 1997, P 39.
6. "Hydraulic Pumps," Aerospace Engineering, May, 1997, P 38.
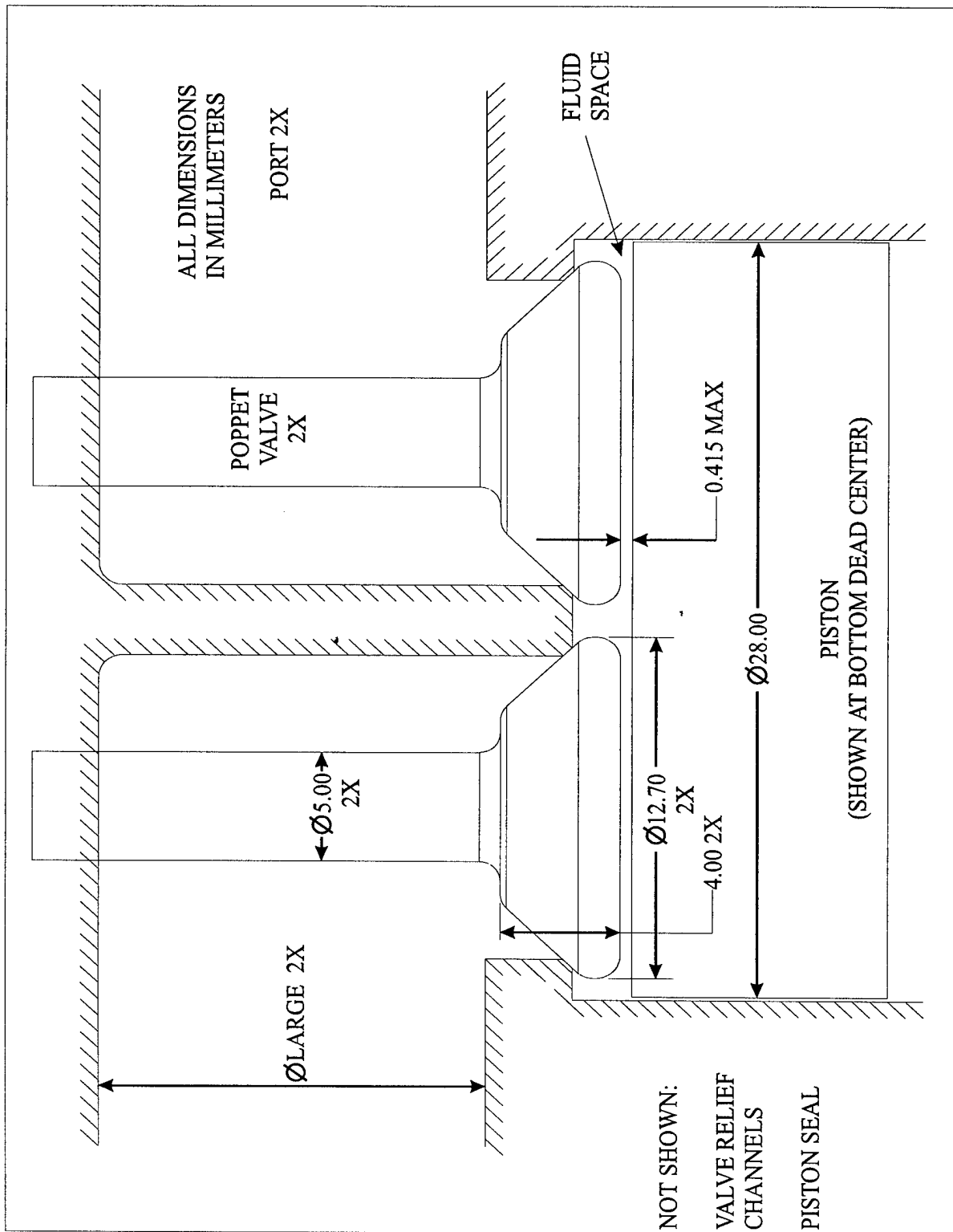
Figure II-1. Pump fluid chamber configuration.
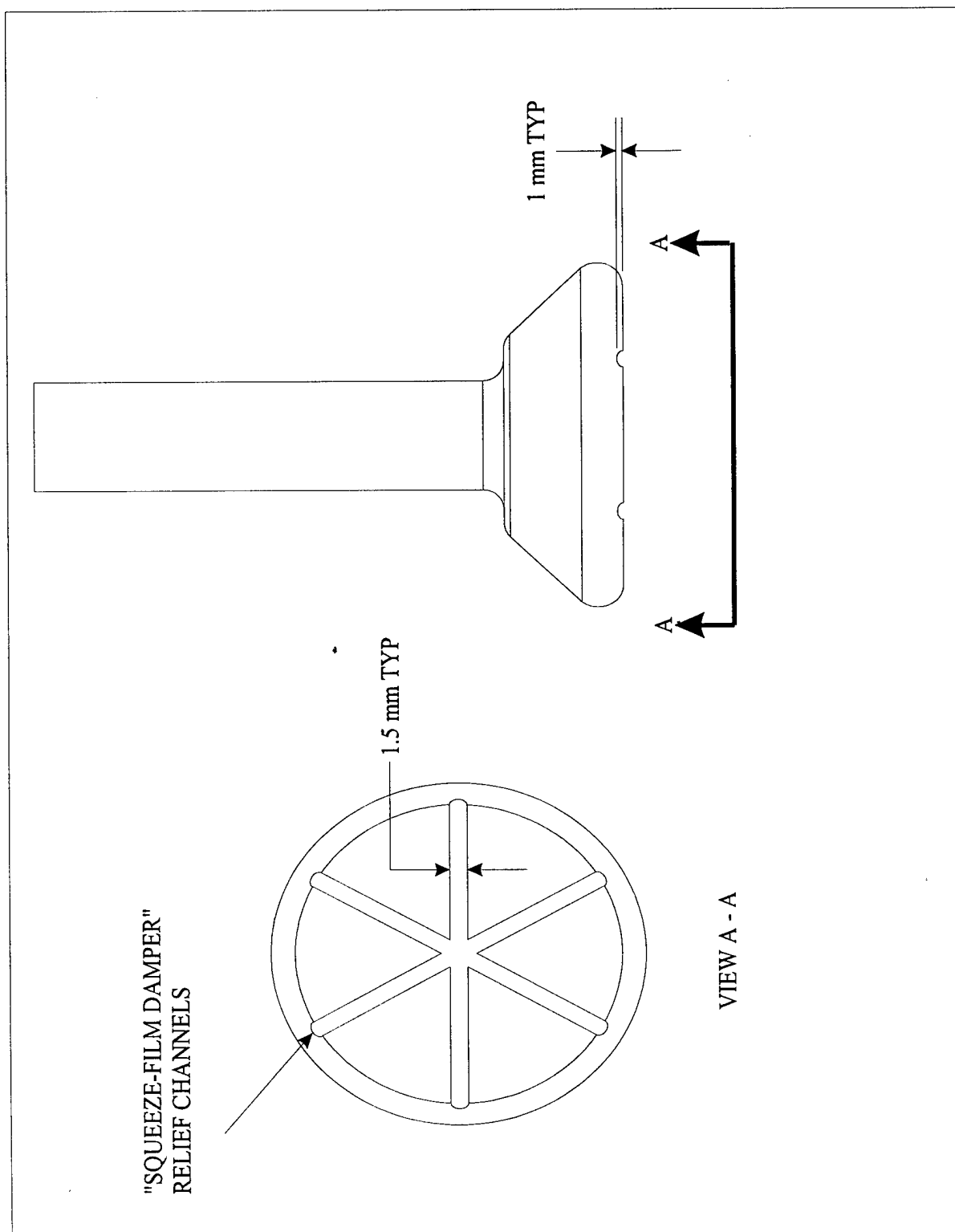
Figure II-2. Detail of poppet valve flow channels.

The pump piston and valves are each operated by their own transducers, which are not shown. Transducer parameters for the dynamic model are provided by the lumped parameter model. With the transducer parameters chosen, force and displacement from the transducers are determined as a function of electrical input. The dynamic model then integrates the force and displacement loads imposed by the fluid undergoing pressurization with the force and displacement from the pump piston and valve. The integration of the transducer and fluid loads provides a means to determine the size requirements in order to obtain the desired pressure and flow.

The software vehicles chosen for model development are "Simulink," a block diagram package, and "Matlab," a numerical programming package, both available from The Math Works, Inc. Simulink offers the ability to model complex interactions graphically with included and user-defined function inputs from Matlab. The lumped parameter TERFENOL-D magnetostrictive transducer model written in Matlab provides the input to the IEA pump dynamic model in Simulink. The interaction between the software platforms allows the user to determine and design transducers for varying conditions. Specific transducer designs are then integrated into the dynamic model to determine performance characteristics. Both Matlab and Simulink provide a means to model a complete dynamic system to provide overall pump performance information.

A lumped parameter transducer model which provided characteristics of the TERFENOL-D driver was created using Matlab. Magnetic bias was incorporated into the model as discrete magnets inserted between TERFENOL-D rod sections to form a "stack." Although a stack configuration results in a longer coil (and IEA) with proportionally more heat and power dissipated, a uniform magnetic field throughout the volume of TERFENOL-D is much more readily achieved, maximizing its output. In this report, the real power numbers resulting from the model include a conservative estimate of hysteresis and eddy current losses in the transducer stack itself. Specifically, the model calculates eddy current losses for an assumed solid rod of TERFENOL-D. This result should be the upper limit because the TERFENOL-D in the stack is laminated and the stack consists of 68% TERFENOL-D and 32% magnet with a 40% higher magnet material electrical resistivity. Resulting transducer characteristics from the lumped parameter model were implemented in the dynamic model of the pump created in Simulink.

The dynamic model consisted of the pump transducer, fluid interactions, and valve transducers. The pump transducer was driven with an AC voltage which produced a displacement of the piston. Pressure in the pump chamber was determined by the velocity of the pump piston and the flow rate into and out of the pump chamber. Valve transducers required complex controls in order to open and close to obtain optimum flow rates. A more detailed description of the dynamic model is located in appendix A.

For the phase I dynamic model, it was initially assumed that the effect of temperature on density, bulk modulus and viscous damping would be significant. A brief study concluded that this was not the case, thus enabling a simpler analysis using density and bulk modulus at a fixed temperature. Chandler Evans conducted a computational fluid dynamics (CFD) analysis on flow through the open poppet valve. This resulted in a "discharge" coefficient C_d as a function of Reynolds number, Re, figure II-3. For model simplicity, an average C_d value was chosen.

In addition to studying the effect of temperature on the fluid interactions, valve and piston interactions were considered in a study on squeeze film damping. Squeeze film damping occurs when fluid is squeezed out from between two flat surfaces approaching each other. As the surfaces approach, viscous damping effects dominate the narrower and narrower channel, with the net result that the approach velocity is slowed given a constant force. Damping effects can be alleviated by introducing channels recessed into the flat surface(s), thus providing an escape route for the fluid.

For the current dynamic model, squeeze film damping did not affect overall output of the device. From information obtained by Chandler Evans' CFD analysis, figure II-4, squeeze film damping was determined to be negligible unless the gap between the piston and valve was less than 75 micrometers. The current dynamic pump model did not produce gap sizes less than 75 micrometers due to the compressive nature of TERFENOL-D. Stand-off distance of the piston is initially set based on the displacement of the piston and valves leaving the smallest gap possible between the surfaces. After the pump starts and is pressurized, pump chamber pressure compresses the TERFENOL-D, thus increasing the gap between the piston and valves. Since the model does not alter the stand-off distance in real time as the pump is running, the gap is always large enough to disregard the effects of squeeze film damping.

Since the piston and active valves do not 'see' any squeeze film damping effects, they can be modeled based on pressure and, in the case of the active valves, return spring interactions. A complete description of the equations used to create the dynamic model is located in appendix A. The piston is driven with sinusoidal AC voltage input. Due to the transducer dynamics when undergoing valve force balance changes (discussed in more detail on page 17), the active valves require a complex control system to operate effectively. This control is beyond the scope of this phase I SBIR program.

After learning more about the complex nature of active valves, a simplified passive valve model was incorporated into the system for comparison. Although passive valves dictate unidirectional flow and require a shuttle valve to port the fluid, the complex control of the active valves would be completely eliminated. The passive valve model was created using flow rate versus pressure differential relationships from passive valves currently being used in a concurrent TERFENOL-D pump project. To obtain required flow rates, multiple passive valves were used in the model. Using a larger valve would reduce the number of valves required, but may increase unswept volume. A study shoud be conducted in phase II to determine what valve configuration would provide the best results.
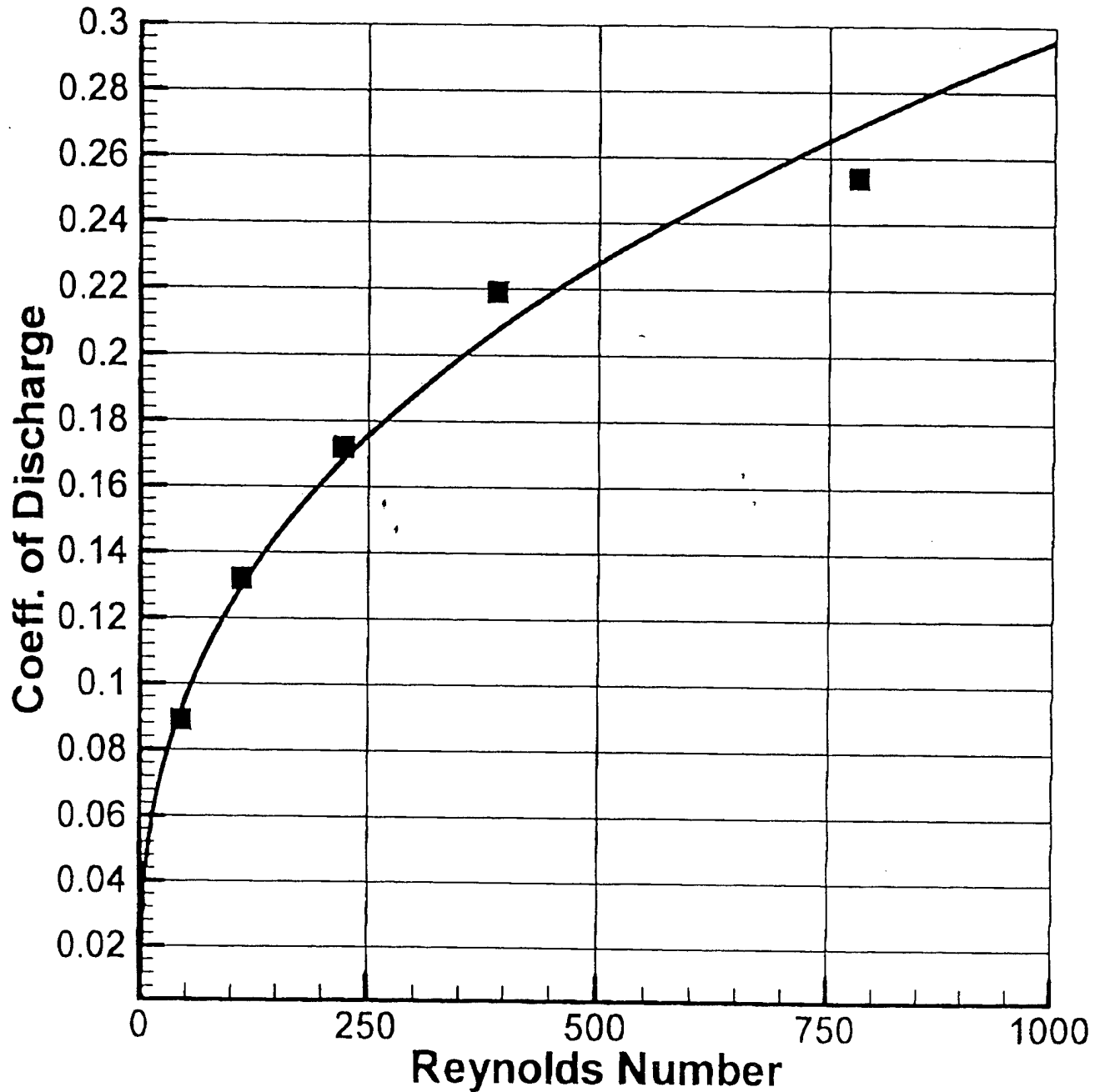
PRESSURE LOSS CHARACTERISTIC

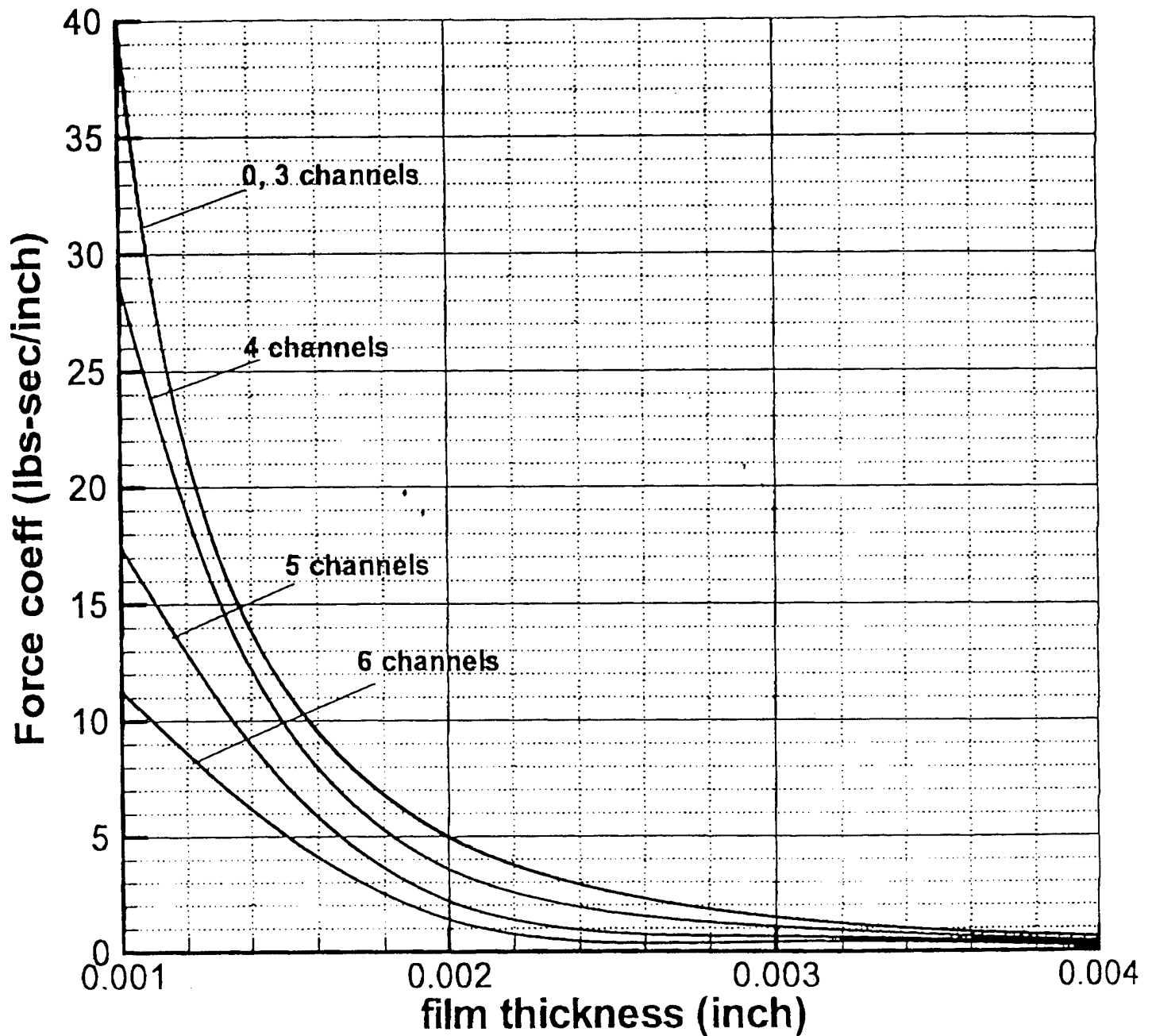Figure II-3. Poppet valve orifice pressure loss characteristic.

SQUEEZE FILM DAMPING

Figure II-4. Squeeze film damping.

To evaluate their effects on power and efficiency, several differential pressures, frequencies, and TERFENOL-D transducer configuration combinations were examined. The following parameters are the final combination of parameters used for both active and passive valve IEA versions except where specifically indicated as active valve parameters. The passive valve information is excluded as too preliminary. Parameters were defined based on the proposal target hydraulic power of one gallon per minute flow rate experiencing a pressure increase of five thousand pounds-force per square inch. Both the phosphate ester hydraulic fluid and the TERFENOL-D were assumed to be at room temperature. Meter-kilogram-second SI units are used due to their convenience with electromechanical transduction.

Overall IEA

Parameter	SI Value (Other Value)	SI Units (Other Units)
Pressure Differential	34.5×10^6 (5,000)	N/m^2 (psi)
Flow Rate	6.309×10^{-5} (1.0)	m^3/s (GPM)
All Component Temperatures	20 (68)	°C (°F)
Fluid	Skydrol or Hyjet Phosphate Ester	
Frequency	400	Hz
Available Voltage	115	Volts rms

Pump Chamber Geometry With Active Valves (See Figures II-1 and II-2)

Active Valve Element

Orifice Flow Coefficient C_d	(See Figure II-3)	dimensionless
Stroke	0.000200	m

Pump Element Transducer

TERFENOL-D Diameter	0.0345	m
TERFENOL-D Length	0.306	m
In-Line Bias Magnet Diameter	0.0345	m
In-Line Bias Magnet Length	0.144	m
Coil Wire Gauge	8	(AWG)
Number Of Coil Layers	2	dimensionless
Number Of Coil Turns	272	dimensionless

Active Valve Element Transducer

TERFENOL-D Diameter	0.021	m
TERFENOL-D Length	0.187	m
In-Line Bias Magnet Diameter	0.021	m
In-Line Bias Magnet Length	0.088	m
Coil Wire Gauge	12	(AWG)
Number Of Coil Layers	2	dimensionless
Number Of Coil Turns	266	dimensionless

III. Relevant Properties of TERFENOL-D

The intermetallic alloy known as "TERFENOL-D" exhibits a useful property termed magnetostriction. That is, it will transduce magnetic energy into elastic energy minus some internal losses. It can be shown that this energy transduction takes place with dimensionless ratio k^2:

$$k^2 = d^2 \times Y^H / \mu^T$$

Perfect, lossless transduction requires that k^2 be unity. For TERFENOL-D, d is the magnetostriction per unit magnetic field intensity, meters per ampere; Y^H is the elastic modulus at constant magnetic field intensity, newtons per square meter; and μ^T is the permeability at constant stress, volt-seconds per ampere-meter. Of these three intrinsic material properties, d and μ^T are well understood and plotted as a function of mechanical compressive stress in figures III-1 and III-2. Only limited data defining Y^H is available. Note that the magnetostriction curves in figure III-1 share a common zero point, thus making the vertical scale relative. If it were an absolute scale, the curves at the different stress levels would be separated vertically with higher stress curves below lower stress curves, thus defining Y^H.

Given the vertical curve separation, it becomes apparent that reducing the stress increase during pressurization then increases displacement, thus showing that there is an optimum stress increase versus displacement relationship to maximize hydraulic power output. "Linearized" d and μ^T values were established by choosing two endpoints and fixing a straight line between them. See table III-1.

The most compelling references listing applicable compliance (the inverse of Y^H) values are Moffett, et al[7] and especially Clark, et al.[8] The Clark reference lists a compliance value for a changing stress level, but the stress level is somewhat over what the IEA is doing. The most useful information from these two references is that the coupling factor k tends to remain in the neighborhood of 0.7, yielding a k^2 of 0.49. From this, Y^H can be inferred. See table III-1. All values in table III-1 except Y^H can be located on figures III-1 and III-2.

These transduction material properties were combined with other fixed material properties, solenoid coil wiring, and the hydraulic requirements to solve for size, preliminary voltage, and current requirements. The results were then treated as input to the Simulink model which then solved for the dynamic operation.

7. Mark B. Moffett, James M. Powers, and Arthur E. Clark, "Comparison of Terfenol-D and PZT-4 power limitations," J. Acoust. Soc. Am. 90 (2), Pt. 1, August 1991, p 1184.
8. A. E. Clark, J.P. Teter, M. Wun-Fogle, M. Moffett, and J. Lindberg, "Magnetomechanical coupling in Bridgman-grown $Tb_{0.3} Dy_{0.7} Fe_{1.9}$ at high drive levels," J. Appl. Phys. 67 (9), 1 May 1990, p 5007.

Figure III-1. Magnetostriction of TERFENOL-D as a function of pre-stress.
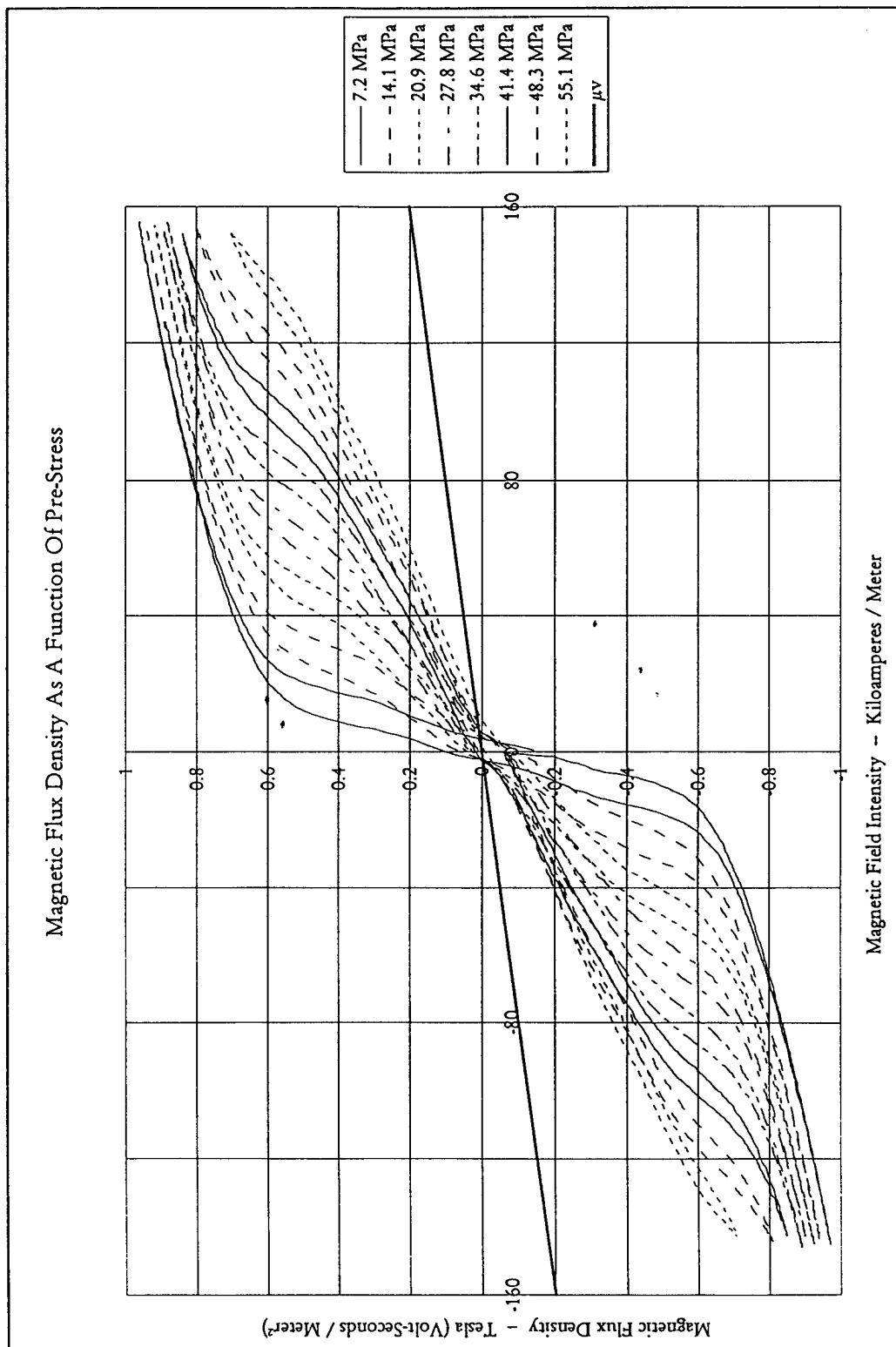
Figure III-2. Magnetic flux density of TERFENOL-D as a function of pre-stress.

Table III-1. Relevant Transduction Values

Low Stress (MPa)	High Stress (MPa)	Low Strain (μm/m)	High Strain (μm/m)	Low Field (kA/m)	High Field (kA/m)	Low Flux Density (V-s/m²)	High Flux Density (V-s/m²)	d ($\times 10^{-8}$ m/A)	μ^T ($\times 10^{-6}$ V-s/A-m)	Y^H ($\times 10^9$ N/m²)	k^2
7.2	27.8	100	1 000	3	88	0.180	0.710	1.059	6.235	27.24	0.49
7.2	20.9	100	1 000	3	70	0.180	0.690	1.343	7.612	20.68	0.49
7.2	14.1	100	1 000	3	55	0.180	0.695	1.731	9.904	16.20	0.49

IV. Results

The target differential pressure of ~5,000 psi was considered as well as an intermediate ~3,600 psi and lower ~2,000 psi differential pressure IEA. In the following tables, the power going into the active valve system consists of only the power required for the piston. (Valve power requirements approximately double the listed electrical input and therefore halve the listed efficiency. For the calculations listed below, valve power is not included. See valve power discussion on page 17.) For the similar cases, preliminary indications are that using passive valves results in a more efficient IEA than using the active valves, even without considering the power required to operate the active valves themselves.

It was determined that 400 hertz operation outperformed 800 hertz operation. At 400 hertz, performance as a function of output pressure rise is predicted to be at about 5,000 psi:

Parameter	SI Value (Other Value)	SI Units (Other Units)
Input Voltage (Pump Only)	124	volts, rms
Input Current (Pump Only)	49	amperes, rms
Electrical Phase Angle	1.3069	radians
Input Power (Pump Only)	1 585 (2.13)	watts (horsepower)
Output Pressure Rise	35.31 (5,121)	MPa (psi)
Output Flow Rate	1.792×10^{-5} (0.284)	m³/s (GPM)
Output Power	632 (0.85)	watts (horsepower)
Power Conversion Efficiency	0.399	dimensionless

At about 3,600 psi:

Parameter	SI Value (Other Value)	SI Units (Other Units)
Input Voltage (Pump Only)	113	volts, rms
Input Current (Pump Only)	39	amperes, rms
Electrical Phase Angle	1.2064	radians
Input Power (Pump Only)	1 571 (2.11)	watts (horsepower)
Output Pressure Rise	24.83 (3,602)	MPa (psi)
Output Flow Rate	2.082×10^{-5} (0.33)	m³/s (GPM)
Output Power	517 (0.69)	watts (horsepower)
Power Conversion Efficiency	0.329	dimensionless

At about 2,000 psi:

Parameter	SI Value (Other Value)	SI Units (Other Units)
Input Voltage (Pump Only)	110	volts peak-to-peak
Input Current (Pump Only)	30	amperes peak-to-peak
Electrical Phase Angle	1.1813	radians
Input Power (Pump Only)	1 253 (1.68)	watts (horsepower)
Output Pressure Rise	14.51 (2,105)	MPa (psi)
Flow Rate	2.713×10^{-5} (0.43)	m³/s (GPM)
Output Power	389 (0.52)	watts (horsepower)
Power Conversion Efficiency	0.310	dimensionless

V. Discussion

Active valve operation turns out to be the single most critical aspect of the overall configuration. Opening the valves at the correct time relative to the pressure versus time curve is critical and opening them the correct distance relative to a desired pressure drop is equally critical. This is a direct result of the IEA configuration itself. Because the valves are poppets, the amount of force the transducers need to exert is directly related to the pressure difference across that valve. Secondly, if the valves are opened too soon, outlet pressure is communicated to the pump piston, resulting in dynamic problems.

Because the transducers themselves introduce an inductive time constant that varies depending on instantaneous mechanical compressive stress and magnetic field intensity, controlling the voltage waveform to obtain the desired dynamics requires careful attention to physical subtleties. Increasing frequency raises the required voltage to maintain the same mechanical waveform amplitude. This is because the allowable rise time for current (which converts to magnetic field intensity) is reduced, thus necessitating higher voltage.

The transducer sizing was optimized for speed, lowest power consumption, etc. While the pump and valve transducers were sized individually, integrating their interactions required developing a valve electrical input control methodology based on a feedback parameter and scheme. Because of the way TERFENOL-D works, transducers optimized in this manner displayed increased sensitivity to force changes and therefore complicated the control scheme.

At the beginning of a valve opening stroke, the magnetic field intensity within the transducer begins to build. Through TERFENOL-D's magnetoelastic response, the increasing intensity changes the force balance within the transducer by overcoming the spring pre-load and any force due to pressure differential across the valve poppet. Once this occurs, the valve poppet begins to move. At the same time, the pump piston is very quickly changing the pressure differential across the poppet. Therefore, the mechanical compressive bias of the valve transducer is also being changed due to externally imposed change in pressure forces.

The changing force balance across the valve poppet changes the mechanical compressive bias on the TERFENOL-D which in turn changes the magnetic permeability. (Note that the lumped parameter approach that was modeled implicitly assumes that the force balance changes evenly in time and space throughout the entire volume of the TERFENOL-D, an assumption subject to increasing error with speed due to the finite speed of an elastic wave through the underdamped material.) Changes in permeability reflect back into the electrical side of the device, requiring very fast voltage slew rates to maintain correct current flow. While the solution to the closed valve problem is relatively straightforward, what happens when the valve opens is more complicated. Now the open poppet is subjected to hydrodynamic forces that also interact with the pump piston transducer.

An integrator to determine the valve transducer input electrical power used was not coded into the model. Instead, an estimate of total power was made based on graphs of voltage and current versus time.

To resolve whether or not active poppet valves merited further pursuit, a valve operation profile was fixed and it was assumed that the valves could be operated to this profile. Then the pump pressure versus valve interaction dynamics were removed from the overall IEA operation to evaluate total performance. The results with the active valves were much lower than expected. The passive valves gave preliminary indications of better performance.

VI. Conclusions

The IEA is feasible! There is no advantage to using active valves. The analysis performed in phase I was unable to show a performance increase justifying their increased power consumption. While the IEA concept holds much inherent potential, the results reveal that extensive foundation work remains to be done before an effective, optimized IEA can be built. Maximum energy density transducer designs have limitations imposed by the TERFENOL-D transducer material itself as well as the configuration attempting to take advantage of that energy. As a result of the software predictive models, several invaluable lessons have been learned at this early stage of the design process, thus reducing the ultimate cost of building an economical device.

Obtaining hydraulic output power is the reason for building an IEA. During the study, the lessons learned collectively manifested themselves as lower than desired available hydraulic output power. They include:

1) Modeling has made it clear that operational frequency is one of the most critical parameters governing size and therefore weight and cost. There are two major factors that limit frequency.

    Active valve operation frequency and therefore pump maximum frequency is subjected to valve transducer frequency limitations. This is because it must open quickly. Power usage is high and controllability becomes increasingly difficult with frequency.

    The second frequency limit is imposed by fluid flow parameters. This program has not yet explored the upper limits imposed by inertia, compliance, and fluid viscosity.

2) Hydraulic pressure rise across the pump has a significant effect on pump transducer size and of course weight, power, and cost.

3) The coefficient of discharge C_d, appears to be low due to the active valve configuration.

4) Carrying out the work on this program has made it clear that simplifying the transduction parameters results in transducers exhibiting non-optimum size, weight, power consumption, and cost. This is most evident at the preferred high mechanical compressive bias and high magnetic field intensity bias where the simplifications no longer hold true. Phase II will use the full transduction equations to optimize the transducer(s).

5) Lumped parameter modeling refinements in the area of eddy current effects were not incorporated due to time. After building and de-bugging the numerical models for this program, a superior method of predicting the effects of eddy currents and stacked magnets became available.

6) Because the IEA is an inductive device, periodically applying voltage without letting the current drop back to zero results in an offset current. That is, the inductive time constant keeps current circulating under certain operational scenarios. The result is unnecessary heat, lower displacement, and displacement offset.

VII. Recommendations

The goal of demonstrating the feasibility of the IEA concept has been shown by the results of this program and by the results of ancillary commercially-funded efforts. It is recommended that this program be extended into phase II. The phase II objectives are to complete trade-off decisions that will enhance performance, robustness, and reliability, plus the design, fabrication, and testing of a prototype IEA that, following phase III design for manufacturing, will be suitable for integration into flight, land, or marine vehicles. These decisions clearly include a much more thorough analysis of passive valve incorporation and the effects of higher frequency on fluid dynamics.

Appendix A

Fluid Model Development

Modeling the complete pump system is imperative in designing the optimum transducer. Interactions between piston displacement, pressurization, valve action, and fluid flow determine the constraints placed upon the transducers and geometry of the system. Initially, the pump geometry and fluid flow are created separately from the TERFENOL-D transducer design. Once each model was proven to be accurate, the transducer model was integrated into fluid model. Upon integrating the two models, the effect of varying pressure differential in the pump chamber could be seen in the altered performance of the transducers. The transducers were then modified to create an optimum design.

Fluid Model

Fluid modeling began with creating a model to accurately show the pressurization and expansion of the fluid inside the pump chamber with no valve action taking place. For simplicity in adding valve action, pressure within the chamber was determined by the net flow rate of fluid.

$$\dot{P} = \beta \frac{A_1 \dot{x}_1}{V}$$

<div align="right">Equation A-1</div>

Instantaneous pressure is a function of bulk modulus and flow rate based on piston displacement, area, and chamber volume. Pressure was then integrated with time to obtain total pressure with in the pump chamber. After determining that the chamber was pressurizing correctly, given a sinusoidal displacement of the piston, the valves were activated and additional flow rate terms added to the pressure in equation A-1.

$$\dot{P} = \beta \frac{A_1 \dot{x}_1 + q}{V}$$

<div align="right">Equation A-2</div>

Pressure was now based on the total flow rate in the pump chamber. Inflow was added to and outflow was subtracted from the flow rate created by piston displacement. Flow rate through the open poppet valves was determined based on turbulent orifice flow where C_d is the flow coefficient, ρ is density of the fluid, A is the area of the restriction and ΔP is the pressure differential across the valve.

$$q = C_d A_2 \sqrt{\frac{2\Delta P}{\rho}}$$

<div align="right">Equation 3</div>

After the fluid model was proven to be capable of pressurizing and flowing in and out of the valves, the TERFENOL-D transducer model was tested.

TERFENOL-D Transducer Model

The model described above was tested with currently existing transducer characteristics to determine model accuracy. Given a square wave input, the displacement and current response was typical with ringing occurring at each step. Settings for the proposed transducer in the pump system were also tested and produced similar ringing as a response to square wave input. Confidence in the TERFENOL-D transducer model was established and integration into the fluid model began.

Equations of Motion

To integrate the TERFENOL-D transducers into the system model, equations of motion for the piston and valves were determined. The piston was taken as a simple mass with a pressure force from the fluid opposing the force of the TERFENOL-D transducer. Using the mass and displacement of the piston, represented by m_1 and x_1 respectively, the following equation was derived.

$$\ddot{x}_1 = \frac{1}{m_1}\left(F_{t1} - P_1 A_1\right)$$

Equation 4

Where A_1 is defined as the area of the piston and P_1 is the pressure within the pump chamber.

The poppet valves require a spring to hold the valve shut against pressure when it is not in operation. Also, pressure is present on both sides of the valve rather than just one side as was the case with the piston. With the mass and displacement of the valve, m_2 and x_2 respectively, the following equation of motion is obtained.

$$\ddot{x}_2 = \frac{1}{m_2}\left(F_{t2} - P_1 A_2 + P_2 A_2 - k_2(x_2 + x_{20})\right)$$

Equation 5

Where A_2 is defined as the area of the valve, P_1 is the pressure with in the pump chamber, P_2 is the pressure with in the line, k_2 is the spring constant and x_{20} is the initial compression of the spring. Note that $k_2 x_{20}$ must be sufficiently strong to hold the valve shut at the highest foreseen pressure differential within the system.

Once the transducer and fluid models were integrated, optimum TERFENOL-D driver, pump chamber and valve geometries were determined to obtain target flow rate and pressure differentials with minimum power usage. In addition, optimum control of the valve system increased flow into and out of the pump chamber.